Available online at www.sciencedirect.com
SCIENCE DIRECT
Journal of Power Sources 144 (2005) 204–207
JOURNAL OF POWER SOURCES
www.elsevier.com/locate/jpowsour

Short communication

Electrochemical reaction of lithium with Zn_3P_2

M.V.V.M. Satya Kishore, U.V. Varadaraju *

Materials Science Research Centre and Department of Chemistry, Indian Institute of Technology Madras, Chennai 600036, India

Received 16 August 2004; accepted 20 November 2004
Available online 28 April 2005

Abstract

Zn_3P_2 has been studied as an anode material for lithium-ion batteries. Electrochemical studies demonstrate that the initial discharge and charge capacities are 1056 and 710 mAh g^{-1}, respectively. The discharge–charge reaction mechanism of lithium with Zn_3P_2 is analyzed by ex situ X-ray diffraction. On initial discharge, LiZn alloy is formed in a matrix of Li_3P. Upon charge, LiZn alloy is transformed completely into Zn metal and Li_3P is converted partially to P, which reacts with Zn to form the original Zn_3P_2 phase. The reversible capacity of Zn_3P_2 is improved when cycled in the limited voltage window.

Keywords: Lithium-ion battery; Zn_3P_2; Anode; Specific capacity

1. Introduction

Current research on lithium batteries is focused on new anode materials to obtain higher specific capacities than those given by the currently used carbon. Several lithium alloys such as Li–Sn, Li–Al and Li–Si exhibit high capacity, but capacity retention is limited because of large volume changes during charge–discharge cycling [1,2]. Attempts have been made to overcome this problem by exploiting intermetallic materials that contain electrochemically active material embedded in an inactive matrix [3–7]. Recently, considerable attention has been devoted to phosphides because of their ability to react with large amount of lithium at low potentials. Transition metal phosphides such as MnP_4 [8], CoP_3 [9,10], FeP_2 [11], CuP_2 [12], Li_2CuP [13], Li_9TiP_4 [14,15], and Cu_3P [16,17] have been studied as anode materials for Li-ion batteries. It is interesting to note that the reaction of lithium with phosphides involves different mechanisms. Depending on the structure and composition, the transition metal present in the phosphides acts as a spectator or it is involved in new phase formation and transformations. In MnP_4 [8], a reversible phase transformation is observed, wherein P–P bonds are cleaved during discharge to give antifluorite Li_7MnP_4, which is reversible on charge and forms the original layered MnP_4 structure. In CoP_3 [9,10], however, the structure collapses completely on discharge to produce nanophase cobalt metal embedded in a matrix of Li_3P. The Li_3P is electrochemically active and the lithium can be reversibly extracted to leave either LiP or P. In CuP_2 [12], the copper metal formed on lithium insertion gives a new phase Li_2CuP during charge. The counter cation present in the transition metal phosphides does not take any lithium. Zinc metal is known to react with lithium reversibly [18,19] and several zinc based oxides and intermetallics have been examined as anode materials for Li-ion batteries [20–23]. This has stimulated the present investigation of Zn_3P_2 as an anode material for Li-ion batteries to exploit the reversible capacity due to both Zn and P.

2. Experimental

Zn_3P_2 was synthesized at high temperatures in an evacuated sealed quartz tube from stoichiometric amounts of zinc and red phosphorus. The reactants were heated at 450 °C for

* Corresponding author. Tel.: +91 44 2257 8256; fax: +91 44 2257 0509.
E-mail address: varada@iitm.ac.in (U.V. Varadaraju).

0378-7753/$ – see front matter © 2005 Published by Elsevier B.V.
doi:10.1016/j.jpowsour.2004.11.060

24 h and then at 700 °C for 24 h and cooled to room temperature. The heating and cooling rates were 1 °C per min. The product was ground and pelletized. The pellets were reheated in an evacuated sealed quartz tube at 750 °C for 24 h.

Identification of the phases and phase purity were confirmed by powder X-ray diffraction (XRD) (Rich-Seifert, Germany, Cu Kα radiation). Lattice parameters were calculated by using the AUTOX program.

Electrochemical studies of Zn_3P_2 were performed in two-electrode Swagelok cells. The weight ratios of the active material, acetylene black (Denka Singapore Pvt. Ltd.) and polyvinylidene fluoride used in making the composite electrodes were 45:45:10 and 80:10:10. A thick slurry of the respective mixtures was made by using *n*-methyl-2-pyrrolidinone and was then coated on a stainless-steel foil. Prior to cell assembly, the electrodes were heated in an oven at 100 °C for 12 h. The swagelok cells were assembled in an argon-filled glove box (mBraun, Germany, <5 ppm H_2O) and used lithium metal (Aldrich, 0.75 mm thick, 99.9%) as a counter electrode, Teklon (Anatek, USA) as the separator and 1 M $LiPF_6$ in 1:1 EC + DMC (Chiel Industries Ltd., Korea) as the electrolyte. Galvanostatic charge–discharge cycling of the cells at room temperature was undertaken between fixed voltage limits and at the C/5 rate by means of an Arbin battery cycling unit (Arbin BT 2000, USA).

At various lithiated and delithiated states, electrochemical cells were disassembled inside the glove box and the electrodes were covered with a mylar film and their XRD patterns were obtained.

3. Results and discussion

The powder X-ray diffraction pattern of Zn_3P_2, shown in Fig. 1, indicates the formation of single phase and all the peaks are indexed according to the JCPDS file no. 22-1021. The tetragonal lattice parameters calculated by least squares fitting are $a = b = 8.07(1)$ Å and $c = 11.42(6)$ Å.

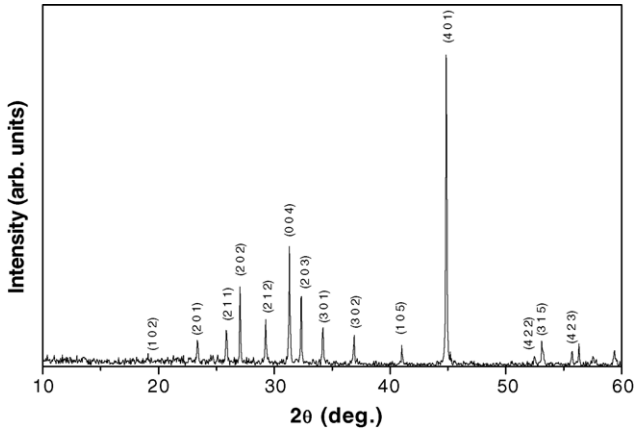

Fig. 1. Powder X-ray diffraction pattern of Zn_3P_2.

The initial discharge and charge curves of Zn_3P_2 electrode made with 10 wt.% and 45 wt.% acetylene black are presented in Fig. 2. The high acetylene black content causes an increase in charge capacity. This is due to the increase in the electronic conductivity of the matrix. Therefore, in the present work, the electrochemical studies of Zn_3P_2 with 45 wt.% acetylene black will be examined. During initial discharge, the voltage falls from the open-circuit voltage (2.8 V) to 1.0 V. A small plateau is observed at ∼0.8 V, followed by a long plateau at ∼0.5 V. The initial step at 0.8 V not only involves the intercalation of lithium into acetylene black, but also the formation of a solid electrolyte interphase (SEI) layer. The formation of a SEI with carbon has also been observed for a CoP_3 electrode made with 40 wt.% carbon [9]. After subtracting the capacity due to acetylene black, the initial discharge capacity of Zn_3P_2 is 1056 mAh g^{-1}. This corresponds to reaction of ∼10 Li. The charge profile is similar to that of discharge and the voltage increases smoothly to a plateau at 0.65 V. The initial charge capacity to 1.5 V is 710 mAh g^{-1}, which corresponds to the extraction of 6.8 Li and a faradaic efficiency of about 67%.

The reaction mechanism of lithium with Zn_3P_2 during the first cycle has been identified by recording ex situ XRD patterns of the electrodes at selected voltages, i.e., stages a to h in Fig. 2. The XRD patterns are shown in Fig. 3. Although the capacity up to 0.60 V is 280 mAh g^{-1} (∼2.7 Li), there is no predominant change in the XRD pattern. This clearly indicates that the initial discharge capacity is due to the intercalation of lithium into acetylene black. The same also holds true for a Li/Zn_3P_2 cell made with 10 wt.% acetylene black, for which the plateau at 0.8 V is absent. The XRD pattern (a) shows that the peak positions of Zn_3P_2 remain unchanged during discharge down to 0.60 V. There is however, a decrease in the intensities with slight broadening of the peaks, as well as a small peak at ∼43° that is characteristic of the (1 0 1) reflection of elemental Zn and indicates the extrusion

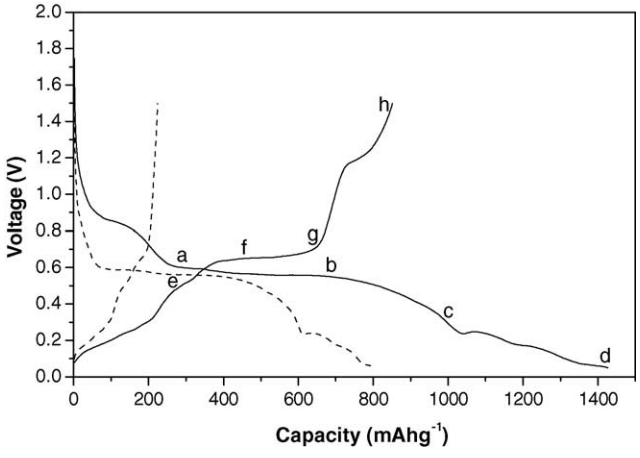

Fig. 2. Initial discharge and charge profiles of Zn_3P_2 with 45 wt.% acetylene black (—) and 10 wt.% acetylene black (---) at C/5 rate in the voltage window 0.05 to 1.5 V.

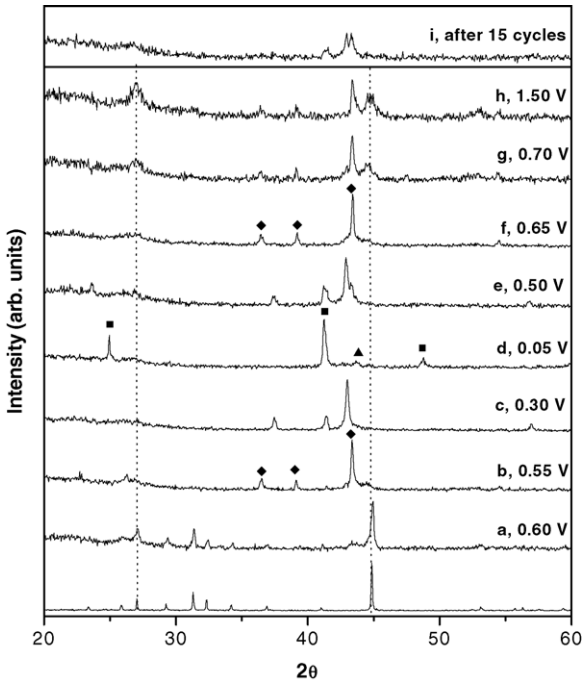

Fig. 3. Ex situ XRD patterns of Zn_3P_2 electrode during first cycle at different voltages. Peaks marked with ♦, ■, and ▲ are assigned as Zn, LiZn and Li_3P phases, respectively.

of Zn from the lattice. Zn_3P_2 has a defect anti-fluorite structure, in which one-quarter of the metal sites are vacant [24]. Although the structure has vacancies, it is not stable towards lithium intercalation. The XRD pattern at 0.55 V exhibits the presence of sharp peaks that correspond to the formation of Zn metal. Thus, the capacity up to 0.55 V is due to the reaction of lithium with phosphorus. The Zn_3P_2 phase peaks have completely disappeared and this indicates structural collapse and the presence of Zn metal in the Li–P matrix. There is no evidence of the formation of any intermediate ternary phases such as LiZnP. On further discharge, Zn reacts with lithium to form Li_xZn alloy. Zinc can react with lithium to form an alloy of maximum composition LiZn [18]. The XRD pattern at 0.30 V shows the presence of both LiZn alloy and Zn. The peak at ~37.5° may be due to the formation of an intermediate Li_xZn phase, where $x < 1$. The transformation of Zn to LiZn alloy involves several phases such as $LiZn_4$, Li_2Zn_5, $LiZn_2$ and Li_2Zn_3 [18]. The emergence of these phases has been observed in an in situ XRD study of a Zn_3N_2 electrode [25]. The fully-discharged state of Zn_3P_2 shows the presence of LiZn and Li_3P. The XRD features of Li_3P are very weak and suggests the formation of nanoparticles. Overall, the discharge mechanism is attributed to two steps that can be written as:

$$Zn_3P_2 + 3xLi \rightarrow 3Zn + (2-x)P + xLi_3P (0 \leq x \leq 2) \quad (1)$$

$$3Zn + 3Li \rightarrow 3LiZn \quad (2)$$

According to the above reactions, the maximum consumption of lithium should be 9. The observed capacity (~10 Li), however, is higher than this theoretical value. The excess capacity can be attributed to the formation of a SEI.

On charge, lithium is extracted initially from the LiZn alloy to form elemental Zn. The XRD pattern during charge at 0.5 V shows the presence of both LiZn and Zn phases, and at 0.65 V lithium is extracted completely from LiZn. On further charge, lithium is extracted from Li_3P and the phosphorus formed reacts simultaneously with Zn metal to yield the original Zn_3P_2 phase. This behaviour is confirmed by the XRD patterns taken at 0.7 and 1.5 V, wherein the peaks at 2θ ~27° and ~45° are characteristic of a Zn_3P_2 phase. The degree of crystallinity of Zn_3P_2 is poor. The charge mechanism can be ascribed as follows:

$$3LiZn \rightarrow 3Zn + 3Li \quad < 0.65\,V \quad (3)$$

$$\left.\begin{aligned} &2Li_3P \rightarrow 6Li + 2P \\ &3yZn + 2yP \rightarrow yZn_3P_2 \ \ (0 \leq y \leq 1) \end{aligned}\right\} > 0.65\,V \quad (4)$$

From XRD studies, it is clearly evident that LiZn alloy is completely reversible during charge. A capacity loss is observed, however, and indicates the limited reversibility of extraction of Li from Li_3P. Hence, the charge capacity observed (~7 Li) is less than the theoretical value (9 Li). The return to a Zn_3P_2 phase indicates that a structural relationship need not exist between the product (LiZn and Li_3P) and parent structures. Recently, this feature was observed in Cu_3P [16], wherein the Cu, Li_2CuP and Li_3P formed during discharge are reversible on charge and reform crystalline Cu_3P. With InSb, a partial return of original phase was observed after charge [26]. Although, no comment was made on this behaviour, it was clearly evident from the in situ XRD study that the pattern for the charged electrode shows the presence of a small amount of InSb phase, which was absent in the fully-discharged pattern.

The differential capacity plots for the first two cycles of Zn_3P_2 are shown in Fig. 4. A peak in the derivative curve represents a plateau in the voltage profile. The peak voltages

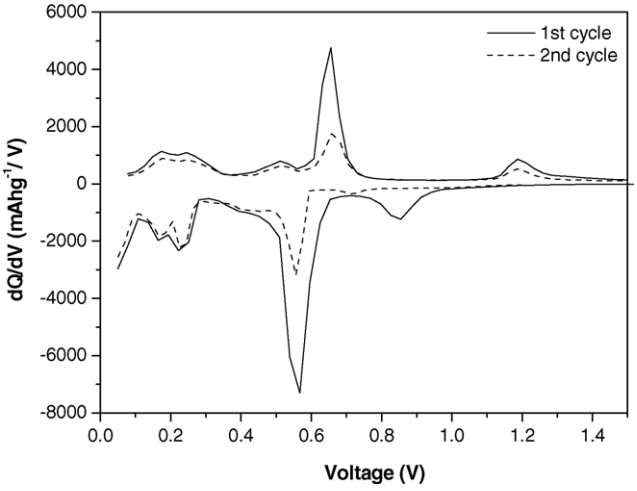

Fig. 4. Differential capacity plots of Zn_3P_2 for first two cycles.

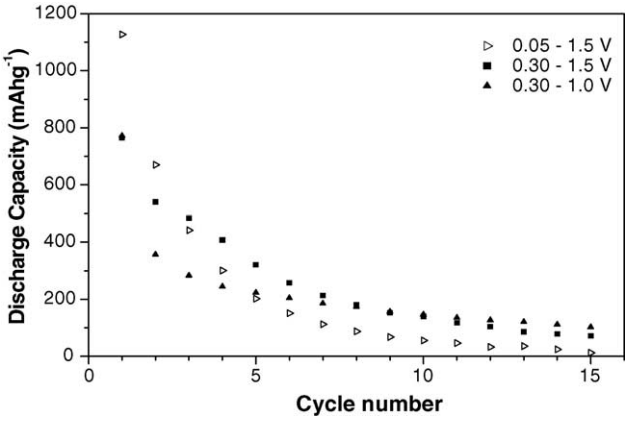

Fig. 5. Discharge capacity vs. cycle number of Li/Zn_3P_2 cells cycled in voltage windows 0.05 to 1.5 V, 0.3 to 1.5 V and 0.3 to 1.0 V at C/5 rate.

in the first two cycles are identical, which indicates that the reaction mechanism followed during the initial cycle is repeated in the second cycle. This shows that Zn_3P_2 formed during the first charge reacts with lithium at nearly in the same potential during the second discharge.

The cycling performance of Zn_3P_2 conducted over the voltage windows of 0.05 to 1.5 V, 0.3 to 1.5 V and 0.3 to 1.0 V is given in Fig. 5. The reversible capacities observed in the voltage windows 0.3 to 1.5 V and 0.3 to 1.0 V are predominantly due to the reversibility of Li_3P. The reversible capacity cycled in the voltage window 0.05 to 1.5 V is poor and there is a small improvement in the capacity retention when cycled in the voltage window 0.3 to 1.0 V. The value after 15 cycles is $\sim$100 mAh g^{-1}. The reversible capacity reported by the zinc-containing compounds Zn_3N_2 and Zn_4Sb_3 is also very poor [25,23]. For Zn_4Sb_3, however, cycling performance is enhanced by milling the material with graphite. In the present study, cracks are observed in the cycled Zn_3P_2 electrode, which indicate volume changes during cycling. The XRD pattern of a discharged electrode after 15 cycles (0.05 to 1.5 V window) is shown in Fig. 3(i). The presence of unreacted Zn_3P_2 and Zn in the discharged electrode suggests that cracking leads to the disconnection of particles. Milling with carbon and/or nanophase Zn_3P_2 could possibly improve the cycling performance.

4. Conclusions

The discharge and charge profiles of Zn_3P_2 exhibit a plateau at $\sim$0.6 V. An ex situ XRD study has revealed the formation of bulk zinc metal during the initial stages of discharge and on complete discharge, LiZn alloy and Li_3P are formed. During charge, LiZn converts back to Zn at low voltages and extraction of lithium from Li_3P at above 0.65 V leads to the re-formation of Zn_3P_2. Although Zn_3P_2 provides high reversible capacity during the first cycle, the cycling stability is poor. A discharge capacity of $\sim$100 mAh g^{-1} is observed after 15 cycles, with a voltage window 0.3 to 1.0 V. Zn_3P_2 is an attractive alternative anode material because of low polarization and also due to the reaction of lithium at similar potentials during initial and successive cycles.

References

[1] J.O. Besenhard, J. Yang, M. Winter, J. Power Sources 68 (1997) 87–90.
[2] R.A. Huggins, J. Power Sources 81/82 (1999) 13–19.
[3] M.M. Thackeray, J.T. Vaughey, C.S. Johnson, A.J. Kropf, R. Benedek, L.M.L. Fransson, K. Edstrom, J. Power Sources 113 (2003) 124–130.
[4] O. Mao, J.R. Dahn, J. Electrochem. Soc. 146 (1999) 423–427.
[5] L.Y. Beaulieu, J.R. Dahn, J. Electrochem. Soc. 147 (2000) 3237–3241.
[6] L.M.L. Fransson, J.T. Vaughey, K. Edström, M.M. Thackeray, J. Electrochem. Soc. 150 (2003) A86–A91.
[7] R. Alcántara, F.J. Fernández-Madrigal, P. Lavela, J.L. Tirado, J.C. Jumas, J. Olivier-Fourcade, J. Mater. Chem. 9 (1999) 2517–2521.
[8] D.C.S. Souza, V. Pralong, A.J. Jacobson, L.F. Nazar, Science 296 (2002) 2012–2015.
[9] V. Pralong, D.C.S. Souza, K.T. Leung, L.F. Nazar, Electrochem. Commun. 4 (2002) 516–520.
[10] R. Alcántara, J.L. Tirado, J.C. Jumas, L. Monconduit, J. Olivier-Fourcade, J. Power Sources 109 (2002) 308–312.
[11] D.C.C. Silva, O. Crosnier, G. Ouvrard, J. Greedan, A. Safa-Sefat, L.F. Nazar, Electrochem. Solid State Lett. 6 (2003) A162–A165.
[12] K. Wang, J. Yang, J. Xie, B. Wang, Z. Wen, Electrochem. Commun. 5 (2003) 480–483.
[13] O. Crosnier, C. Mounsey, P. Subramanya Herle, N. Taylor, L.F. Nazar, Chem. Mater. 15 (2003) 4890–4892.
[14] M. Morcrette, F. Gillot, L. Monconduit, J.-M. Tarascon, Electrochem. Solid State Lett. 6 (2003) A59–A62.
[15] F. Gillot, M.P. Bichat, F. Favier, M. Morcrette, M.L. Doublet, L. Monconduit, Electrochim. Acta 49 (2004) 2325–2332.
[16] O. Crosnier, L.F. Nazar, Electrochem. Solid State Lett. 7 (2004) A187–A189.
[17] H. Pfeiffer, F. Tancret, M.-P. Bichat, L. Monconduit, F. Favier, T. Brousse, Electrochem. Commun. 6 (2004) 263–267.
[18] J. Wang, P. King, R.A. Huggins, Solid State Ionics 20 (1986) 185–189.
[19] Z. Shi, M. Liu, J.L. Gole, Electrochem. Solid State Lett. 3 (2000) 312–315.
[20] H. Li, X. Huang, L. Chen, Solid State Ionics 123 (1999) 189–197.
[21] F. Belliard, P.A. Connor, J.T.S. Irvine, Solid State Ionics 135 (2000) 163–167.
[22] R. Alcántara, M. Tillard-Charbonnel, L. Spina, C. Belin, J.L. Tirado, Electrochim. Acta 47 (2002) 115–120.
[23] G.S. Cao, X.B. Zhao, T. Li, C.P. Lu, J. Power Sources 94 (2001) 102–107.
[24] A.D. Izotov, V.P. Sanygin, V.F. Ponomarev, Kristalografiya 23 (1978) 764–767.
[25] N. Pereira, L.C. Klein, G.G. Amatucci, J. Electrochem. Soc. 149 (2002) A262–A271.
[26] K.C. Hewitt, L.Y. Beaulieu, J.R. Dahn, J. Electrochem. Soc. 148 (2001) A402–A410.